Design of single-material guided-mode resonance filter

Xiaoyong Fu (傅小勇)[1,2*], **Kui Yi (易 葵)**[1], **Jianda Shao (邵建达)**[1], **and Zhengxiu Fan (范正修)**[1]

[1]*Shanghai Institute of Optics and Fine Mechanics, Chinese Academy of Sciences, Shanghai 201800*

[2]*Graduate University of Chinese Academy of Sciences, Beijing 100049*

*E-mail: masfxy@163.com

Received May 20, 2008

In this letter, a guided-mode resonance (GMR) filter with the same material for both the grating layer and the waveguide layer is designed, and its optical properties are investigated. The GMR filter owns almost 100% reflection at the resonance wavelength of 800 nm with the full-width at half-maximum (FWHM) of 20 nm, and its sideband reflection from 700 to 1000 nm is less than 5%. As the resonance wavelength is influenced by more than one parameter during the fabrication process, GMR filter with the same resonance wavelength can be obtained by adjusting other parameters or even one parameter to deviate from the design value.

Guided-mode resonance (GMR) filters consisting of diffractive elements and waveguide layers have been extensively studied in recent years[1−4]. At resonance, the wave diffracted by the grating structure couples with the waveguide layer and efficient energy exchange between the reflected and transmitted waves occurs in small parameter ranges (just like wavelength, incidence angle, refractive index, etc.)[5]. Theoretical analysis shows that GMR filters can be designed to exhibit narrow linewidth and low sideband reflection over an extended wavelength region[6,7], which is promising in the applications of laser cavity reflectors, polarizers, switching devices, light modulators, band-pass filters, etc.[1]. Magnusson's team designed single-layer GMR filters with single film material and multi-layer GMR filters with different materials for film and grating layers[5,6,8]. Wang *et al.* reported multi-channel GMR Brewster filters with different materials for grating layers and waveguide layers[1]. Although most of the researches in this filed were theoretical analysis[1−11], several experimental results of the GMR filters have also been obtained[12−14].

In this letter, a GMR filter with the same material for the grating layer and the waveguide layer is designed. This kind of GMR filter can avoid the material change at the grating/waveguide interface and owns fewer defects during the fabricating process, which results in a higher laser damage threshold and can be potentially applied in high-power laser system[15]. By decreasing the material species, this kind of GMR filter is easier to be fabricated. The influence of the fabrication deviation on the GMR filter's optical characteristics is also investigated.

Figure 1 shows a general GMR filter structure with a grating layer and a waveguide layer. The grating layer is a period structure consisting of the film materials with the refractive indices of n_{gL} and n_{gH}, the waveguide layer is a homogenous layer with the refractive index of n. According to the effective index theory, the effective index n_{eff} of the grating layer can be approximately calculated by[5]

$$n_{\mathrm{eff}} = \left[(1-f)n_{\mathrm{gL}}^2 + f n_{\mathrm{gH}}^2 \right]^{1/2}, \tag{1}$$

where f is the grating filling factor.

Considering the GMR structure in Fig. 1 with a TE-polarized incident wave, when a plane wave is incident on the grating layer, it will be diffracted by the grating structure and divided into multiple diffracted orders and the diffracted waves will couple with the waveguide layer. The electric field distribution inside the grating region can be expressed by[5,16]

$$\frac{\mathrm{d}E_i^2(z)}{\mathrm{d}z^2} + \left[k_0^2 n_{\mathrm{eff}}^2 - k_0^2 (n_c \sin\theta - i\lambda/\Lambda)^2 \right] E_i(z)$$

$$+ k_0^2 \Delta\varepsilon \sum_{h=1}^{\infty} \frac{\sin(h\pi f)}{h\pi} \left[E_{i-h}(z) + E_{i+h}(z) \right] = 0, \quad (2)$$

where $E_i(z)$ is the y-component of the electric-field amplitude of the ith order diffracted wave, λ is the wavelength, k_0 is the wave number which equals to $2\pi/\lambda$, θ is the incidence angle, $k_0(n_c\sin\theta - i\lambda/\Lambda)$ is the x-component of the wave propagation index in the grating region, $\Delta\varepsilon = n^2 - n_c^2$, where n_c is the refractive index of the cover media, i is the integer diffracted-order index, and h is the integer Fourier harmonic index. To simplify the equation, the coupling term is ignored and the coupled-wave equation can be reduced to

$$\frac{\mathrm{d}E_i^2(z)}{\mathrm{d}z^2} + [k_0^2 n_{\mathrm{eff}}^2 - k_0^2 (n_c \sin\theta - i\lambda/\Lambda)^2] E_i(z) = 0. \tag{3}$$

Considering the waveguide layer of the GMR structure, the electric field distribution of the wave propagating in the waveguide can be expressed by[16]
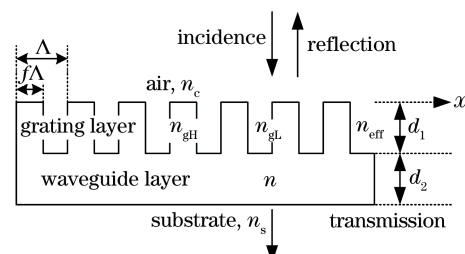
Fig. 1. General structure of a GMR filter consisting of a grating layer and a waveguide layer.

© 2009 Chinese Optics Letters

$$\frac{\mathrm{d}E^2(z)}{\mathrm{d}z^2} + \left[k_0^2 n^2 - \beta^2\right] E(z) = 0, \tag{4}$$

where β is the propagation constant of the mode supported by the waveguide structure.

GMR will occur when a diffracted wave is phase-matching to a wave mode which is supported by the waveguide layer. From Eqs. (3) and (4), if

$$\beta = k_0(n_c \sin\theta - i\lambda/\Lambda), \tag{5}$$

the ith wave diffracted by the grating will propagate in the waveguide guide. And if $i = 1$ or -1, the evanescent wave will strongly couple to the zero-order wave and a complete energy exchange will occur between the forward and backward waves.

According to the slab waveguide theory[17,18], for TE mode, β can be calculated by

$$\tan(\kappa d_2) = \frac{\kappa(\gamma + \delta)}{\kappa^2 - \gamma\delta}, \tag{6}$$

where $\kappa = (n^2 k_0^2 - \beta^2)^{1/2}$, $\gamma = (\beta^2 - n_{\mathrm{eff}}^2 k_0^2)^{1/2}$, $\delta = (\beta^2 - n_s^2 k_0^2)^{1/2}$, d_2 is the thickness of the waveguide layer, n_s is the refractive index of the substrate.

From Eq. (6), when d_2 varies for $\Delta d = \pi/\kappa$, waves with different modes (just like TE$_1$, TE$_2$ modes) can also propagate in the slab waveguide layer.

Equations (5) and (6) present the relationship among the resonance wavelength λ, the grating period Λ, and the waveguide thickness d_2 for the GMR phenomena. Based on the two equations, GMR filters can be designed by choosing proper parameters (just like Λ, d_2, n, f, etc.) for a given resonance wavelength λ. Figure 2 shows the relationship of λ, Λ, and d_2 with the modes of TE$_0$, TE$_1$, and TE$_2$ for the GMR filters.

We designed a GMR filter with the same material for the grating layer and the waveguide layer. The resonance wavelength was designed as 800 nm, and the refractive indices of the cover media n_c, the film material n, and the substrate n_s were chosen as 1.0, 2.0, and 1.52, respectively. The incident angle θ was 0°. Treating the grating layer as a homogenous layer with the effective index of n_{eff}, antireflection (AR) coating design method[19,20] can be used to decrease the sideband reflection of the GMR filter. In this letter, V-coating method is used, which
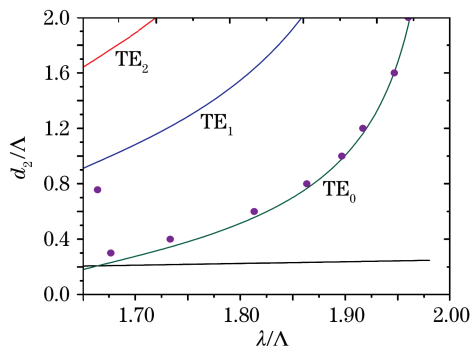
is satisfied by selecting the thicknesses of the layers equal to a quarter of the resonance wavelength. The refractive indices satisfy the condition

$$n^2/n_{\mathrm{eff}}^2 = n_s/n_c. \tag{7}$$

The effective index $n_{\mathrm{eff}} = 1.62$ can be calculated by Eq. (7), and the grating filling factor $f = 0.5439$ can be calculated from Eq. (1). The grating layer thickness $d_1 = 123$ nm and the waveguide layer thickness $d_2 = 100$ nm can be calculated by $d_1 = \lambda/(4n_{\mathrm{eff}})$ and $d_2 = \lambda/(4n)$, respectively. The grating period $\Lambda = 480$ nm can be calculated by Eq. (6).

Rigorous coupled-wave analysis (RCWA) method, which is an exact electromagnetic grating diffraction model providing purely numerical solutions, was used to simulate the reflection spectrum of the proposed GMR filter using the calculated parameters. The result is shown as the dotted line in Fig. 3.

It is found that for the calculated parameters, the resonance wavelength is 773 nm, a little different from the designed wavelength of 800 nm. This may be because of the coupling term in Eq. (2) is ignored and Eq. (2) needs to be amended for our model. This approximation causes the resonance wavelength shifting and the resonance wavelength calculated from Eq. (6) is only a rough value. Accurate value calculated by RCWA method is shown in Fig. 2. It is found that for a given resonance wave, the value of λ/Λ calculated by RCWA method is smaller than the rough data. Based on the original design, just by increasing Λ to 500 nm, the GMR filter with the resonance wavelength of 800 nm is achieved, and its spectrum is illustrated in Fig. 3 as the solid line. This GMR filter owns almost 100% reflection at the resonance wavelength of 800 nm with full-width at half-maximum (FWHM) of 20 nm, and its sideband reflection from 700 to 1000 nm is less than 5%.

GMR filters can be fabricated by thin-film fabrication method and the laser- or electron-beam etching technologies. Deviations during the fabrication process will cause the resonance wavelength shifting. Figure 4 shows the influence of the etching thickness on the resonance wavelength shifting. With the same total thickness of the grating layer and the waveguide layer, a change of 10 nm in the grating thickness will result in the resonance wavelength shifting of 8 nm and over etching will result in

Fig. 2. Relationship among the waveguide thickness d_2, grating period Λ, and resonance wavelength λ for a GMR filter with different modes. Solid dots are results calculated by RCWA method.
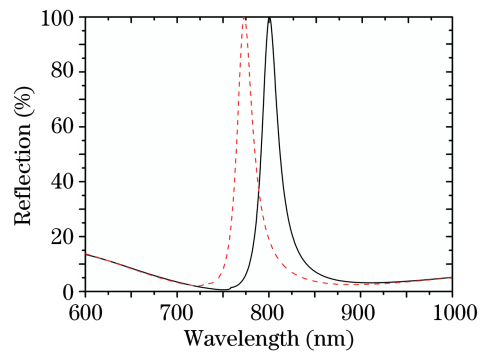
Fig. 3. Reflection spectra of the GMR filters. The parameters are $\theta = 0$, $n_c = 1.0$, $n = 2.0$, $f = 0.5439$, $d_1 = 123.3$ nm, and $d_2 = 100$ nm. The dotted line is the design from Eq. (6) with $\Lambda = 480$ nm, and the solid line is the modified design with $\Lambda = 500$ nm.
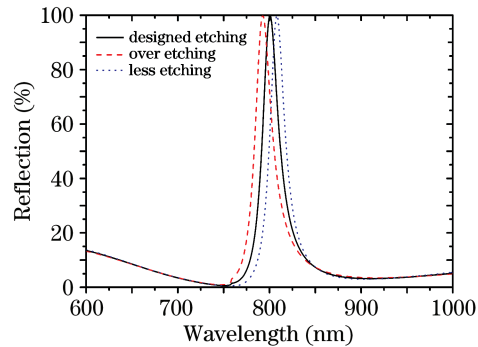
Fig. 4. Reflection spectra of the GMR filters for the cases of designed etching ($d_1 = 123.3$ nm), over etching ($d_1 = 133.3$ nm), and less etching ($d_1 = 113.3$ nm). The total thickness ($d_1 + d_2$) keeps the same, and other parameters are the same as those in Fig. 3.
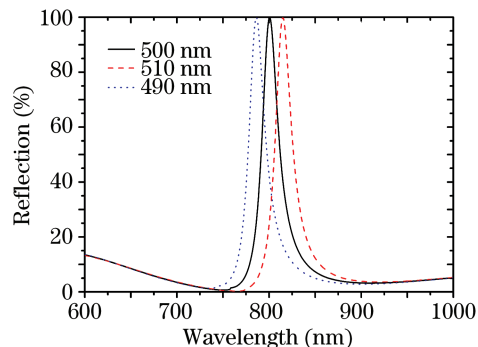
Fig. 5. Reflection spectra of the GMR filters with different grating periods of 490, 500, and 510 nm. Other parameters are the same as those in Fig. 3.

a shorter resonance wavelength. Figure 5 illustrates the GMR filter properties with different grating periods. It can be found that the resonance wavelength will shift 15 nm when the grating period changes 10 nm and the resonance wavelength will increase with the increase of grating period.

For this kind of single-material GMR filter, the resonance wavelength is influenced by more than one parameter, such as grating layer thickness d_1, waveguide layer thickness d_2, grating period Λ, and grating filling factors f. If one parameter deviates from the design value, GMR filter with the same resonance wavelength can also be achieved by slightly adjusting other parameters. For our design, if Λ changes to 490 nm, GMR filter with the same resonance wavelength of 800 nm can also be achieved by adjusting d_1 from 123 to 105 nm, d_2 from 100 to 118 nm, and keeping the rest parameters unchanged.

In conclusion, a GMR filter with the same material for both the grating layer and the waveguide layer was designed. The slab waveguide theory was used to get the rough parameters and RCWA method was used to achieve the accurate parameters. The GMR filter owns almost 100% reflection at the resonance wavelength of 800 nm with the FWHM of 20 nm and its sideband reflection from 700 to 1000 nm is less than 5%. For this kind of single-material GMR filter, even if one parameter deviates from the design value during the fabrication process, the same resonance wavelength can also be achieved by changing other parameters.

References

1. Z. Wang, T. Sang, J. Zhu, L. Wang, Y. Wu, and L. Chen, Appl. Phys. Lett. **89,** 241119 (2006).
2. C. Lenaerts, V. Moreau, Y. F. Lion, and Y. L. Renotte, Opt. Eng. **43,** 2631 (2004).
3. D. W. Dobbs and B. T. Cunningham, Appl. Opt. **45,** 7286 (2006).
4. N. Ganesh, A. Xiang, N. B. Beltran, D. W. Dobbs, and B. T. Cunningham, Appl. Phys. Lett. **90,** 081103 (2007).
5. D. Shin, S. Tibuleac, T. A. Maldonado, and R. Magnusson, Opt. Eng. **37,** 2634 (1998).
6. S. S. Wang and R. Magnusson, Opt. Lett. **19,** 919 (1994).
7. Z. Hegedus and R. Netterfield, Appl. Opt. **39,** 1469 (2000).
8. S. S. Wang and R. Magnusson, Appl. Opt. **34,** 2414 (1995).
9. S. M. Norton, T. Erdogan, and G. M. Morris, J. Opt. Soc. Am. A **14,** 629 (1997).
10. M. G. Moharam and T. K. Gaylord, J. Opt. Soc. Am. **71,** 811 (1981).
11. D. K. Jacob, S. C. Dunn, and M. G. Moharam, J. Opt. Soc. Am. A **17,** 1241 (2000).
12. P. S. Priambodo, T. A. Maldonado, and R. Magnusson, Appl. Phys. Lett. **83,** 3248 (2003).
13. R. Magnusson, D. Shin, and Z. S. Liu, Opt. Lett. **23,** 612 (1998).
14. Z. S. Liu, S. Tibuleac, D. Shin, P. P. Young, and R. Magnusson, Opt. Lett. **23,** 1556 (1998).
15. I. Jovanovic, C. G. Brown, B. C. Stuart, W. A. Molander, N. D. Nielsen, B. Wattellier, J. A. Britten, D. M. Pennington, and C. P. J. Barty, Proc. SPIE **5647,** 34 (2004).
16. R. Magnusson and S. S. Wang, Appl. Phys. Lett. **61,** 1022 (1992).
17. S. S. Wang and R. Magnusson, Appl. Opt. **32,** 2606 (1993).
18. Y. Sun and J. Pan, Chin. Opt. Lett. **5,** 86 (2007).
19. X. Fu, S. Wang, D. Deng, K. Yi, J. Shao, and Z. Fan, Chin. Opt. Lett. **4,** 247 (2006).
20. D. Wang, Z. Fan, J. Huang, J. Bi, and Y. Wang, Chin. Opt. Lett. **4,** 675 (2006).